Formic Acid Adsorption on Dry and Hydrated TiO_2 Anatase (101) Surfaces by DFT Calculations

A. Vittadini,*,† A. Selloni,*,‡,|| F. P. Rotzinger,*,§ and M. Grätzel§

CSSRCC-CNR, via Marzolo 1, I-35131 Padova, Italy, Department of Physical Chemistry, 30 quai E. Ansermet, CH-1211 Geneva, Switzerland, and Institut de Photonique et Interfaces, E.P.F.L. - CH-1015 Lausanne, Switzerland

Received: October 7, 1999

The adsorption of formic acid and sodium formate on the stoichiometric anatase (101) surface has been studied by means of density functional calculations with a slab geometry. On the clean surface, the most stable adsorption structure for HCOOH is a molecular monodentate configuration, hydrogen bonded to a surface bridging oxygen, while for HCOONa a dissociated bridging bidentate geometry is preferred. The bidentate chelating structure is energetically unstable for both the acid and the salt. On the hydrated surface, both HCOOH and HCOONa preferentially form an inner-sphere adsorption complex. HCOOH maintains a monodentate coordination, but, due to the interaction with a nearby water molecule, it becomes dissociated, while HCOONa again prefers a bridging bidentate structure. The energies for adsorption from an aqueous solution are estimated to be 0.30 and 0.79 eV for HCOOH and HCOONa, respectively.

I. Introduction

Titanium dioxide, in both the rutile and the anatase forms, is a widely used material for a large variety of applications, ranging from catalysis to photoelectrochemistry.[1,2] However, while rutile (the most stable polymorph) has been extensively investigated in recent years, much less is known about the fundamental physical and chemical properties of anatase. Motivated both by the general interest of molecular adsorption at metal-oxide surfaces and by the crucial role of anatase films in applications such as dye-sensitized solar cells,[3] in this work we consider the adsorption of formic acid on anatase (101), which is the most stable surface for this material,[4] and one of those most frequently exposed in nanoparticles synthesized for solar cells.[5] Interest in formic acid, on the other hand, is motivated by the fact that this is the simplest species containing a carboxylic group, which is often used to bind photosensitizers to these nanoparticles.[3]

The adsorption of HCOOH on the surfaces of TiO_2-rutile—particularly on the most stable (110) surface—has been extensively studied, both theoretically and experimentally. On oxidized rutile (110), it is established that HCOOH dissociates.[6] At saturation, which is attained at $\theta = 1/2$, a (2×1) periodicity is observed by low-energy electron diffraction. Images obtained by scanning tunneling microscopy[7] suggest that formate binds to *two* surface Ti cations in a bridging configuration. This picture has been confirmed by X-ray photoelectron diffraction,[8] as well as by ab-initio slab and cluster calculations.[9,10]

At variance with the case of rutile, experimental information concerning the adsorption of formic acid on anatase is rather limited, and mostly refers to samples exposing various surface planes. Earlier temperature-programmed desorption (TPD) measurements on anatase powders[11,12] found evidence of both molecular and dissociative adsorption of HCOOH. Features associated with both HCOOH and $HCOO^-$ have been observed also in recent attenuated total reflection (ATR)-FTIR experiments of gaseous formic acid adsorption on anatase samples containing mostly (101) and (100) surfaces.[13] In addition, analogous ATR-FTIR measurements indicate that when a solution of HCOOH is titrated (with e.g., NaOH) in the presence of TiO_2-anatase, three species are present: HCOOH(aq), $HCOO^-$ (aq), and $HCOO^-$ (adsorbed).[13] No molecularly adsorbed HCOOH is observed on the hydrated surface, and the maximum amount of $HCOO^-$ is adsorbed at pH 3−5.

In this work we try to make contact with this experimental information by performing calculations for several possible adsorption conformations of formic acid and sodium formate on both the dry and hydrated anatase (101) surfaces. Sodium formate on the hydrated surface, in particular, is studied with reference to the case of a surface in contact with a slightly acidic solution. In fact, it is now widely accepted that the adsorption mode of a molecule on a metal oxide surface is greatly influenced by the presence of secondary interactions, e.g., hydrogen bonds, established by the adsorbate both with the surface and with co-adsorbed species. Therefore, to correctly predict how a molecule is adsorbed, we should consider not only the chemical state and the local coordination of the adsorption site, but also its surface environment. For the case of water adsorption on titania surfaces, for instance, theoretical calculations have found that at low coverage water is *molecularly* adsorbed on anatase (101),[14] while it is *dissociatively* adsorbed on rutile (110),[15] despite the fact that the involved acidic/basic sites are 5-fold coordinated Ti^{4+} cations and 2-fold coordinate bridging O^{2-} anions in both cases. This can be explained in terms of the different hydrogen bonding stabilization of the undissociated vs dissociated adsorbate provided by the different surface structures. Furthermore, adsorbate−adsorbate interactions were shown to play an important role, favoring, on rutile, a mixed molecular and dissociative adsorption at one monolayer coverage.[15] Similar results were found also in a study on methanol adsorption at the rutile (110)

* Corresponding authors.
† CSSRCC-CNR.
‡ Department of Physical Chemistry, Geneva.
§ Institut de Photonique et Interfaces, E.P.F.L.
|| Present address: Chemistry Department, Princeton University, Princeton, NJ 08544.

10.1021/jp993583b CCC: $19.00
Published on Web 01/13/2000

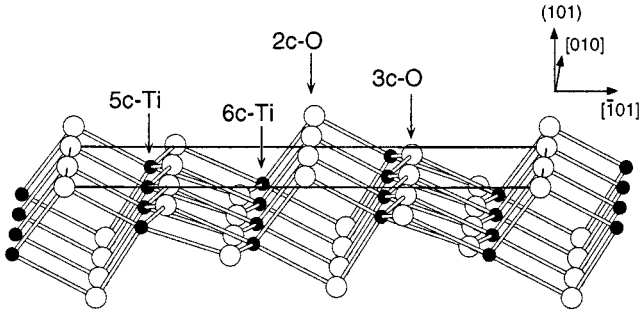

Figure 1. The clean (101) surface. Large empty and small filled circles represent O and Ti atoms, respectively. The dimensions of surface cell used in the calculations, depicted by thin black lines, are (10.24 × 7.57) Å^2. Half of the slab thickness used in the calculations is shown.

surface,[16] suggesting that the interplay of several effects in determining the adsorption mode on oxide surfaces could be a rather general feature when molecules able to form hydrogen bonds are involved.

II. Computational Approach

A. Technical Details. Calculations have been performed using the Car-Parrinello approach, as described in refs 17 and 18. The generalized gradient approximation (GGA) is used for the functional of exchange-correlation[19] as implemented by Dal Corso et al.[20] This approximation of the density functional theory (DFT) has been found to yield satisfactory results in a recent study of adsorption on this[14] as well as on other metal oxide surfaces.[15,21] For C, O, Na, and Ti, electron−core interactions are described by GGA-consistent "ultra-soft" pseudopotentials.[22] Valence states include 2*s* and 2*p* shells for C and O; semi-core 2*s* and 2*p*, together with the 3*s* state, for Na; 3*s*, 3*p*, 3*d* and 4*s* states for Ti. The smooth part of the wavefunctions is expanded in plane waves. A kinetic energy cutoff of 35 Ry was found necessary to adequately describe the properties of the $(HCOOH)_2$ dimer (see below), and was therefore used to describe the adsorption of HCOOH, while a cutoff of 30 Ry was sufficient to study HCOONa adsorption. The cutoff for the augmented electron density is 200 Ry. Due to the large size of our supercell (see below), the k-sampling has been restricted to the Γ point only.

To model the surface, we used a periodically repeated slab geometry. Different slabs are separated by a vacuum ∼9.5 Å wide; each slab is four layers (about 6 Å) thick and comprises 16 TiO_2 units. The supercell includes two surface cells along [010], corresponding to an area of (10.24 × 7.57) Å^2 (see Figure 1). To check the adequacy of our slab thickness, the adsorption of one water molecule was calculated using both the standard and a thicker (∼9.5 Å) slab. A difference in adsorption energy of only 0.02 eV was found between the two cases.

Atomic relaxations were carried out using a damped second-order dynamics until residual forces were less than 0.05 eV/Å. Structural optimizations were frequently followed by short Car-Parrinello molecular dynamics (MD)[17] runs aimed at checking the stability of the calculated structures, and eventually finding more stable minima by relaxing selected configurations generated during the runs. An electronic fictitious mass of 1100 au and a timestep of 7 au (0.169 fs) were used to integrate the equations of motion, with the hydrogen mass set equal to 2 amu. In all calculations, the molecules were adsorbed on the upper surface of the slab only, while the four lowest TiO_2 were kept fixed in their bulk positions.

B. Tests on the HCOOH Molecule and its Dimer. In the gas phase, the isolated HCOOH molecule prefers a conformation

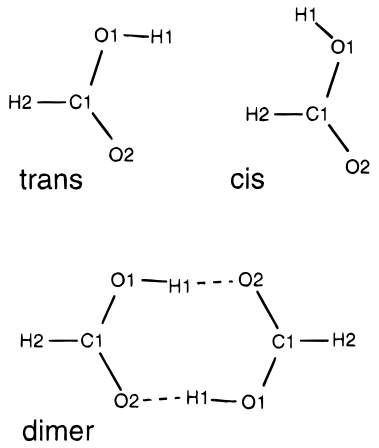

Figure 2. Schematic structures of the monomer and dimer forms of HCOOH.

TABLE 1: Bond Distances (Å) and Bond Angles (deg) for the Gas-Phase HCOOH Species in the Monomeric and Dimeric Forms (experimental values in parentheses[a])

	cis	trans		dimer	
C1−O1	1.37	1.36	(1.36)	1.30	(1.32)
C1−O2	1.21	1.22	(1.22)	1.27	(1.22)
C1−H2	1.12	1.11	(1.11)	1.11	(1.08)
O1−H1	0.99	0.99	(0.98)	1.12	(1.04)
O1′−H1				1.35	
O1−C1−O2	121.8	124.9	(123.4)	126.8	(126.2)
C1−O1−H1	109.4	107.2	(107.3)	111.7	(108.5)

[a] From ref 23.

where the H atoms are in a *trans* position. The *trans* conformer is able to dimerize, forming two intermolecular hydrogen bonds. The structures of these species are depicted in Figure 2, while in Table 1 are reported bond distances and bond angles obtained from our calculations, along with reference experimental data.[23] Our results agree well both with experiment and with other DFT[9,24] and ab-initio[25] calculations. The trans conformer is computed to be more stable than the cis one by 0.13 eV, which is also in agreement with previously published DFT results[24] and with experiment.[26] An important test for our calculations is the evaluation of the dimerization energy, because the hydrogen bonds play an important role in the adsorbate−surface interaction, but are sometimes not well described by DFT. Our computed value (0.84 eV) is in fair agreement with experiment (0.66 eV[27]).

III. Adsorption on the Clean ("Dry") Anatase (101) Surface

On the anatase (101) surface both five-fold and six-fold coordinated Ti atoms (Ti_{5c} and Ti_{6c}) are present, as well as two-fold (O_{2c}) and three-fold coordinated (O_{3c}) oxygens (see Figure 1). Atoms on the relaxed surface are only slightly displaced from their "ideal" positions:[14] the coordinatively unsaturated O_{2c} and Ti_{5c} atoms tend to tighten their bonds with nearest neighbors, and relax inward, by ∼0.06 and ∼0.17 Å, respectively; vice versa, O_{3c} and Ti_{6c} atoms relax outwards, by ∼0.21 and ∼0.11 Å, respectively. This relaxation pattern is qualitatively similar to that predicted by DFT slab calculations for rutile (110).[28,29]

By analogy with other metal-oxide surfaces, including rutile, several different geometries for HCOOH/HCOONa on anatase (101) can be figured out. The coordination may be either *monodentate* (M) or *bidentate* (B), depending on the number

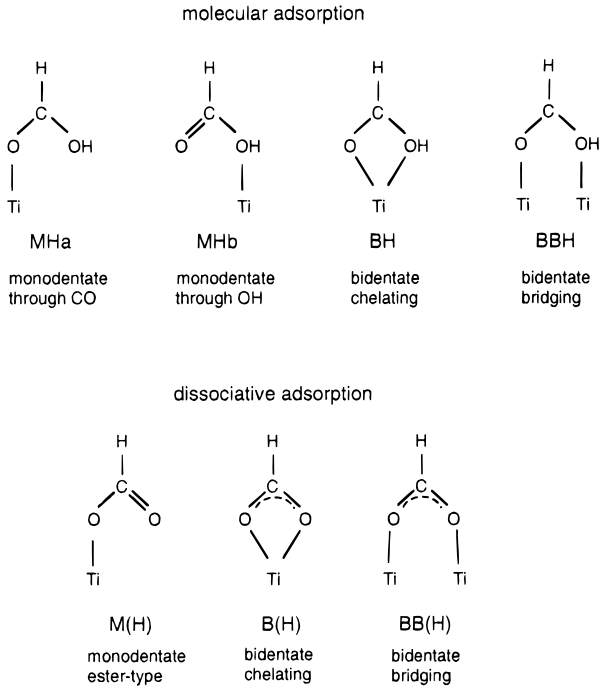

Figure 3. Possible configurations for HCOOH and $HCOO^-$ species bonded to metal cation(s).

TABLE 2: Adsorption Energies (eV), Bond Distances (Å), and Bond Angles (deg) for Various Molecular and Dissociated Conformations of HCOOH and HCOONa on the Dry Anatase (101) Surface[a,b]

geometry	figure	C−O1	C−O2	O1−C−O2	adsorption energy
MHa	4a	1.31	1.24	127.4	0.92
MHb					0.41
BH					not stable
BBH					0.20
M(H)					0.21
B(H)					−0.25
BB(H)	4b	1.28	1.28	128.3	0.68
MNa	5b	1.25	1.31	122.6	1.08
BBNa	5c	1.27	1.29	129.1	1.73

[a] In each supercell four Ti_{5c} sites and a single HCOOH/HCOONa molecule are present. [b] Geometry codes are specified in Figure 3.

of oxygens used by the molecule/anion to coordinate the surface Ti_{5c} acid sites. Furthermore, the bidentate coordination may be either of the chelating or the bridging (BB) type. The possible *molecular* and *dissociated* structures of adsorbed HCOOH are represented schematically in Figure 3 where the abbreviations used to indicate them are also reported. For the molecular species, the monodentate coordination may occur either through the carbonyl group (MHa) or through the hydroxyl group (MHb). Values of the adsorption energies of both HCOOH and HCOONa are summarized in Table 2, together with a few structural parameters (C−O distances and O−C−O angle). For HCOOH, adsorption energies are referred to the isolated trans conformation, even though the most stable form for the free formic acid is the $(HCOOH)_2$ dimer. For HCOONa, adsorption energies are calculated with reference to a hypothetical isolated molecule, in which Na^+ symmetrically bridges the two oxygens of the formate. In all the calculations reported in this section, a single HCOOH/HCOONa molecule per supercell is considered, while four Ti_{5c} sites are available for adsorption.

A. Adsorption of HCOOH. *1. Molecular Adsorption.* For the case of monodentate coordination, preliminary calculations to establish the best orientation for a HCOOH molecule approaching a Ti_{5c} surface site have been carried out. The MHa structure, in which the attack to the cation site occurs through the carbonyl oxygen, is ∼0.5 eV lower in energy than MHb, for which the attack is through the hydroxyl oxygen (see Table 2). This is not surprising, because oxygen prefers a two-fold coordination,[30] while adsorption through the hydroxyl implies the formation of a three-fold coordinated oxygen. Similar conclusions have been obtained in recent theoretical studies on the interaction of HCOOH with the rutile (110)[10] and the ZnO-$(10\bar{1}0)$[31] surfaces.

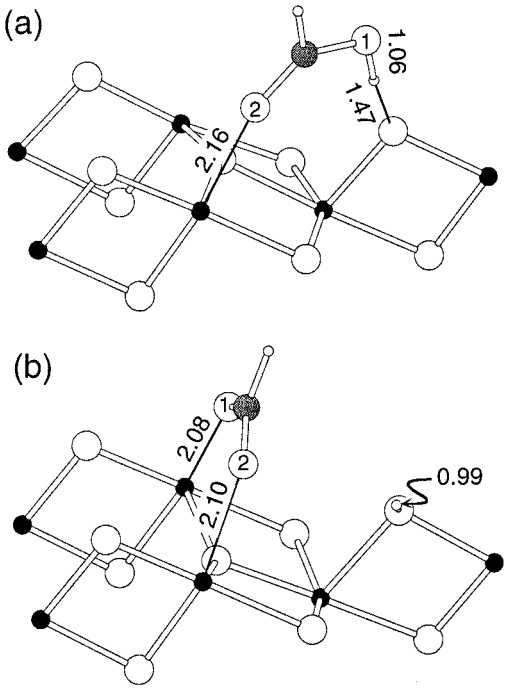

Figure 4. Calculated atomic structures for a HCOOH molecule adsorbed on anatase (101). Ti and O atoms are represented as in Figure 1. Small empty circles represent H atoms, the grey circles represent the C atom. (a) Hydrogen-bonded MHa ester-type molecular state. (b) BB(H) bridging dissociated state.

An important role in stabilizing the MHa structure is played by the hydrogen bond between the hydroxyl proton and a surface bridging O_{2c} atom. As Ti_{5c} and O_{2c} are arranged in pairs on the surface (see Figure 1), two possible configurations can be identified, an "*intra*-pair", where the involved cation and anion belong to the same pair, and an "*inter*-pair" one, where they belong to different pairs. The *inter*-pair arrangement (see Figure 4a), with an adsorption energy of 0.92 eV, is slightly more favorable, by ∼0.02 eV, than the *intra*-pair one. MD simulations (at a temperature of about 100 K) indicate that both these molecular structures are stable, with no tendency to dissociate, thus corresponding to well-defined local minima on the potential energy surface. In both these structures the adsorbed HCOOH molecule has a trans conformation.

Calculations for the bidentate bridging (BBH) and chelating (BH) configurations, where HCOOH is in a cis arrangement, indicate that the BH geometry does not correspond to any local minimum, while BBH has an adsorption energy of only 0.20 eV, so that this structure is largely unfavored with respect to the monodentate MHa one.

2. Dissociative Adsorption. Since no spontaneous dissociation of adsorbed HCOOH was observed to occur during our MD simulations, dissociated configurations were generated by optimizing structures in which the separated H^+ and $HCOO^-$ moieties were placed on suitable sites of the surface. In this case, the bidentate bridging configuration BB(H) (Figure 4b)

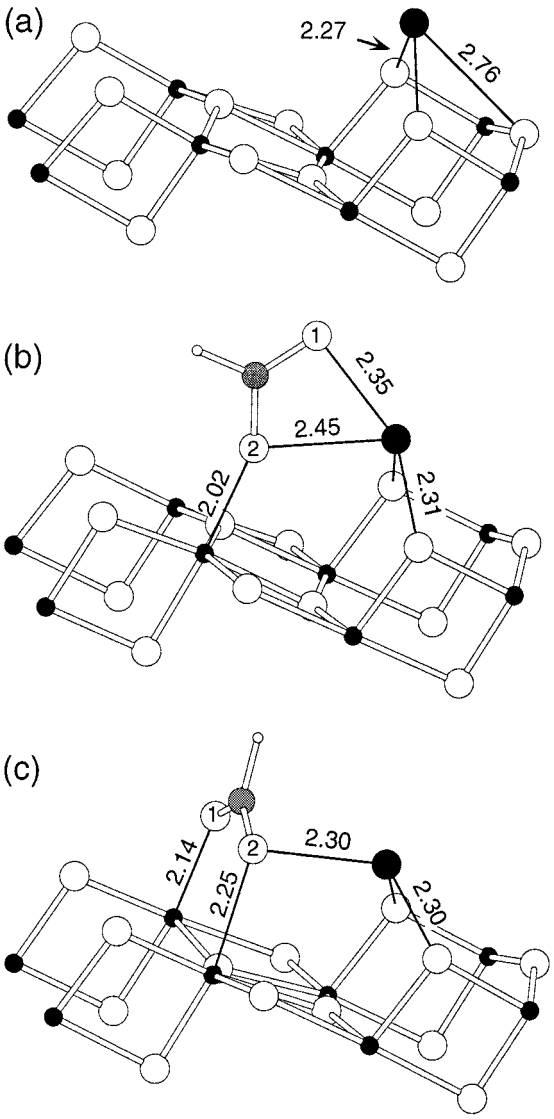

Figure 5. Calculated atomic structures for HCOONa adsorbed on anatase (101). Ti, O, C, and H atoms are represented as in Figure 4, Na^+ is represented by the large filled circle. (a) Isolated Na^+ ion. (b) M(Na) monodentate formate ion. (c) BB(Na) bridging formate ion.

is preferred to the monodentate M(H) one, while the bidentate chelating B(H) geometry correponds to a *negative* adsorption energy (see Table 2). However, the adsorption energy for BB(H) (0.68 eV) is still lower than that for the molecular MHa structure, indicating that, similarly to water,[14] also HCOOH prefers to adsorb molecularly on the dry anatase (101) surface. Although somewhat unexpected (formic acid has a definitely higher gas-phase acidity with respect to water[32]), this result appears consistent with ATR-FTIR experiments on anatase samples exposing mostly (101) and (100) surfaces,[13] as well as with TPD results on anatase powders,[11,12] in which *both* molecular and dissociated configurations of HCOOH were observed. Dissociated configurations may be attributed to surfaces different from the (101) one, as suggested by our recent calculations of water adsorption on (101) and (001) surfaces, where a much higher reactivity for the (001) than for the (101) surface was found.[14] In addition, using Redhead's equation[33] together with the experimental data of refs 11 and 12 and a pre-exponential factor of 10^{13} s^{-1} to obtain an approximate estimate of the desorption barrier for the HCOOH molecule, we find a value of 1.1−1.2 eV, in semi-quantitative agreement with our calculated adsorption energy of 0.92 eV.

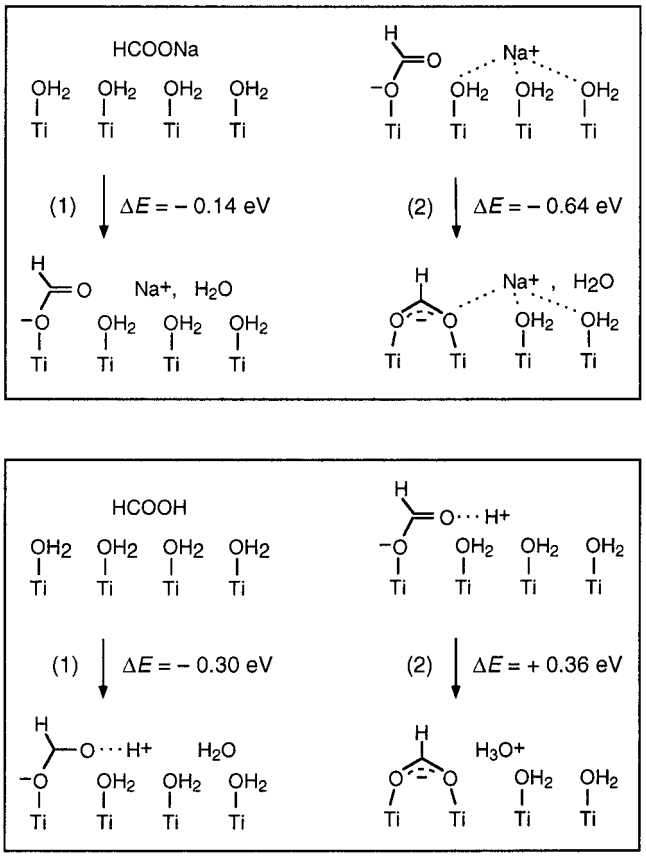

Figure 6. Schematic illustration of the processes in eqs 1 and 2 for HCOONa (upper panel) and HCOOH (lower panel).

A question to ask is why HCOOH dissociates when adsorbed onto other TiO_2 surfaces, particularly on rutile (110), while it prefers to molecularly adsorb on anatase (101). A related issue is the much lower adsorption energy computed for HCOOH on anatase with respect to that reported for rutile (1.94 eV [9]). There are several factors which can contribute to these differences. A frequently used argument when comparing the adsorption geometries and energies of carboxylic acids on different metal oxide surfaces, is the distance between the coordinatively unsaturated cation centers.[34] In the case of TiO_2 surfaces, the 2.96 Å distance on rutile (110) fits the "byte" of the formate ligand in the BB(H) configuration much better than the 3.71 Å value on anatase (101). However, the importance of this effect is not clear-cut, as the topologies of the rutile (110) and anatase (101) surfaces are substantially different. X-ray diffraction structures of titanium oxo clusters show that the distance of Ti centers bridged by carboxylate units usually falls in the 3.0−3.1 Å interval, but distances of ∼3.6 Å have been sometimes observed.[35] To obtain an approximate estimate of the importance of the byte effect, we performed DFT calculations[36] on a simplified cluster model, containing only two Ti_{5c} and one O_{3c} sites, initially in the geometry of the unrelaxed anatase (101) surface.[37] Varying d_{Ti-Ti} (by simply closing the Ti−O−Ti angle) from the value of anatase (101) to that of rutile (110), the formate adsorption energy was found to increase by ∼0.6 eV, arising almost entirely from electronic effects.

Other factors which may be important in determining the difference between rutile (110) and anatase (101) are more difficult to quantify. One possibly relevant effect is the interaction between the BB formate and the backbonds of the O_{2c} oxygens: on rutile (110) the BB formates can be well accommodated in the channels formed by the rows of two-fold coordinated oxygens,[6−10] while this is not true for anatase (101).

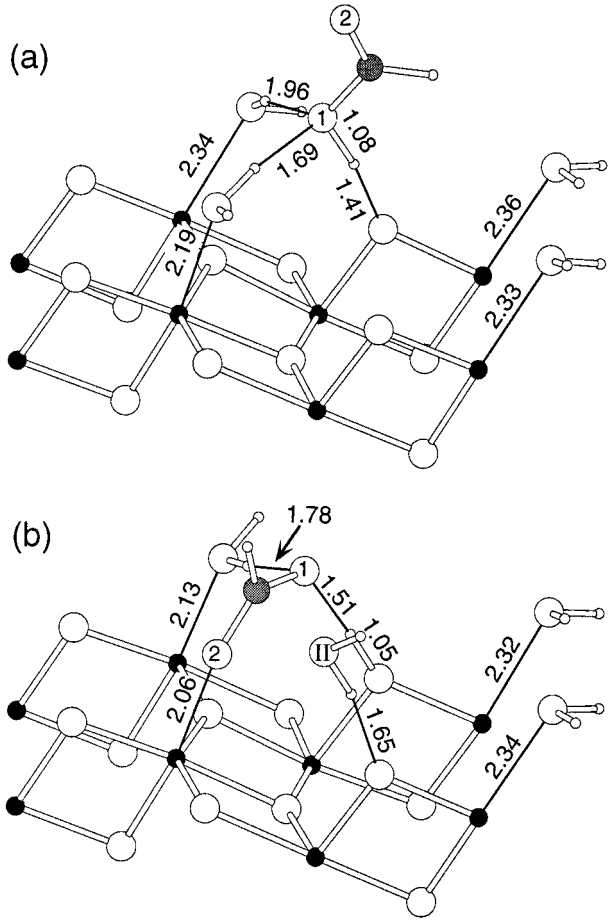

Figure 7. Calculated atomic structures for HCOOH co-adsorbed with four water molecules/supercell on anatase (101). (a) The four H_2O molecules form a full monolayer directly above the surface, the acid is in the second layer; (b) the acid is moved to the first layer in a monodentate form, thus displacing a water molecule to the second layer. For better clarity, the oxygen atom of the second layer water is marked with a roman "II".

Another effect is a larger acidity/basicity of the Ti_{5c}/O_{2c} sites of rutile with respect to anatase. This is likely related to the different structural environments of Ti_{5c} and O_{2c} sites on these surfaces.[2] In particular, we notice that on rutile (110) all nearest neighbors of Ti_{5c} (O_{2c}) sites are 3-fold (6-fold) coordinated oxygens (Ti atoms), while on anatase (101) the surface Ti_{5c} (O_{2c}) sites are coordinated to both O_{2c} and O_{3c} (Ti_{5c} and Ti_{6c}) atoms, resulting in $Ti_{5c}-O_{2c}$ pairs where the coordinatively unsaturated atoms are connected via a bond ~5% shorter than the ideal one.[14]

B. Adsorption of HCOONa. Preliminary calculations for the adsorption of a single Na^+ cation on the clean surface[39] indicate that the most stable adsorption geometry corresponds to a state where Na^+ symmetrically bridges two O_{2c} atoms, and forms also a longer bond with a 3-fold coordinated oxygen (see Figure 5a).[40] Thus, for HCOONa adsorption on the clean surface, we considered an ester-type monodentate (MNa, Figure 5b) and a bridging (BBNa, Figure 5c) configuration, with the Na^+ cation initially placed mid-way between two adjacent O_{2c} sites along [010]. For both configurations, calculated Na−O distances are in the range 2.3−2.5 Å, in agreement with those found in X-ray diffraction studies of sodium formates.[41]

Contrary to the case of HCOOH adsorption, for HCOONa the bridging bidentate BBNa structure, which has *two* bonds with the surface, is preferred (by 0.65 eV) to the monodentate MNa form, which has only one bond (see Table 2).

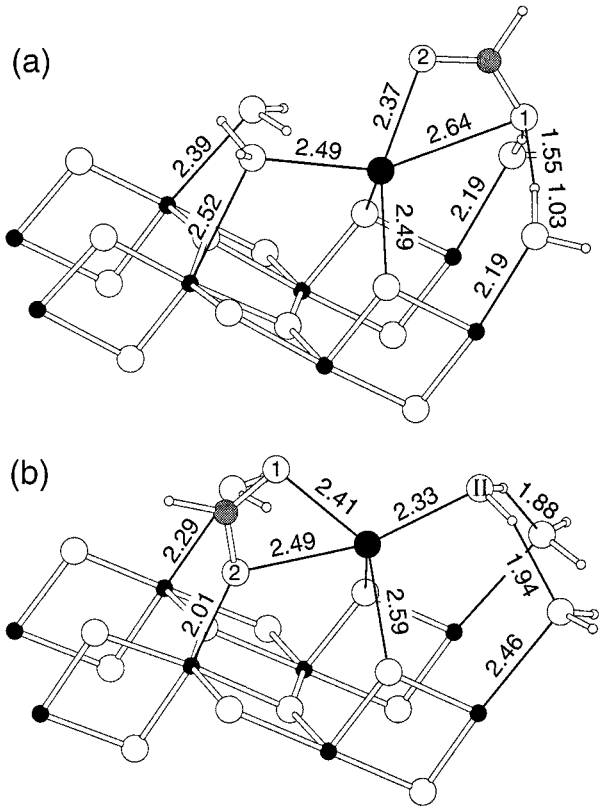

Figure 8. Same as Figure 7, for HCOONa co-adsorbed with four water molecules.

This suggests that in the case of HCOOH the preference for the monodentate structure is mainly related to a weak basicity of O_{2c} sites, making dissociation of the acid unfavorable (remark also the large difference in the adsorption energies for the monodentate dissociated M(H) and undissociated MHa species).

IV. Adsorption on the Hydrated Surface

In this section we present calculations of the energy for adsorbing HCOOH (HCOONa) from an acidic (slightly acidic) aqueous solution onto the anatase surface. In this calculation, we take into account that a water molecule, initially on the surface, is displaced away from it, and similarly, that a HCOOH/HCOONa, initially in solution, is brought onto the surface. In principle, a realistic description of this process would require treating the interface between anatase and liquid water, but this is clearly beyond present computational possibilities for first principles approaches. An attractive alternative would be a hybrid approach in which a quantum-mechanical treatment, for, e.g., HCOOH/HCOONa, the surface, and the water molecules closer to it, is combined with an empirical force field description of water molecules farther away (see, e.g., ref 42, and references therein). However, here we restrict to a simplified model in which only the water molecules of the first layer and some of those in the second layer above the anatase surface are included, while more distant water molecules are completely ignored.

To determine the adsorption structures for HCOOH/HCOONa on the hydrated surface, we have selected and optimized a few likely conformations, involving the monodentate (M) and bridging bidentate (BB) species, plus three or four co-adsorbed water molecules/supercell.[43] We did not consider the bidentate chelating structure which was found to be energetically unstable in the case of a dry surface.

Our first step has been to verify whether HCOOH/HCOONa is adsorbed specifically, forming what is called an inner-sphere

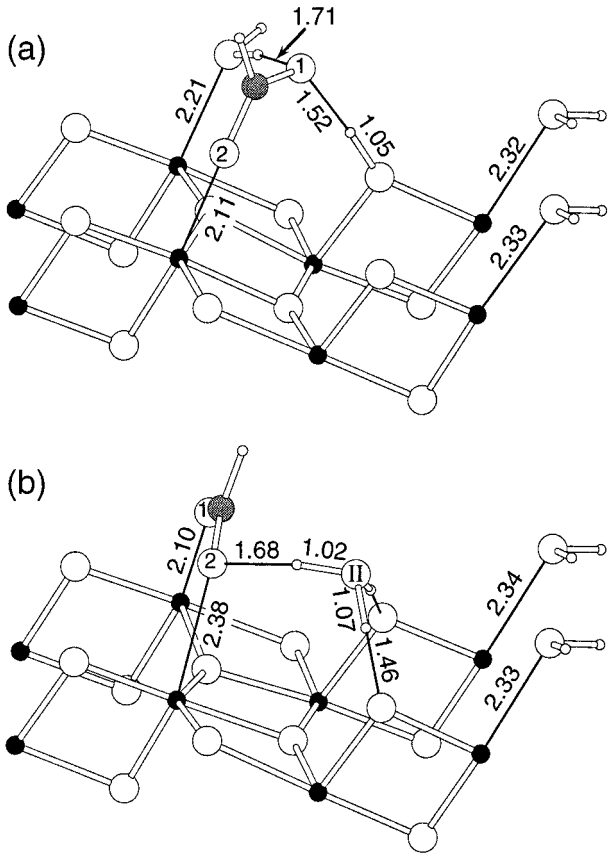

Figure 9. Calculated atomic structures for HCOOH co-adsorbed with three water molecules/supercell on anatase (101). (a) The monodentate M(H)−H_2O structure. (b) The bridging bidentate BB(H)−H_2O form.

adsorption complex (i.e., it prefers staying in the first layer, directly attached to the surface). To this end, we compared the total energies of two geometries involving a HCOOH/HCOONa unit co-adsorbed with *four* water molecules (see Figures 6−8). In the first configuration, the formic acid/formate (coordinated to the sodium cation) is in the second layer. In the second one, the acid/formate is moved to the first layer, and it is singly coordinated to the surface; at the same time a water molecule is diplaced to the second layer according to

$$\text{HCOOH/HCOONa}(2l) + 4\text{H}_2\text{O}(1l) \rightarrow \text{HCOOH/HCOONa}(\text{M}, 1l) + 3\text{H}_2\text{O}(1l) + \text{H}_2\text{O}(2l) \quad (1)$$

where 1*l* and 2*l* denote lst- and 2nd-layer adsorbed species, respectively. We find that this process is *exothermic* by 0.30 and 0.14 eV for HCOOH and HCOONa, respectively. On adsorption, HCOOH dissociates (Figure 7b), and the proton is transferred to the adjacent O_{2c} site.

Next, we consider one HCOOH/HCOONa unit, co-adsorbed with *three* H_2O molecules, and examine the following process:

$$\text{HCOOH/HCOONa}(\text{M}, 1l) + 3\text{H}_2\text{O}(1l) \rightarrow \text{HCOOH/HCOONa}(\text{BB}, 1l) + 2\text{H}_2\text{O}(1l) + \text{H}_2\text{O}(2l) \quad (2)$$

in which the monodentate HCOOH/HCOONa(M,1*l*) configurations transform to bridging bidentate species HCOOH/HCOONa-(BB,2*l*), with one water molecule displaced to the second layer (Figures 6, 9−10). From the adsorption energies on the hydrated surface (Table 3), we can see that, similarly to what found for the dry surface, this process is not energetically favored for HCOOH, whereas it is exothermic by 0.64 eV for HCOONa. This value is almost identical to the energy difference between

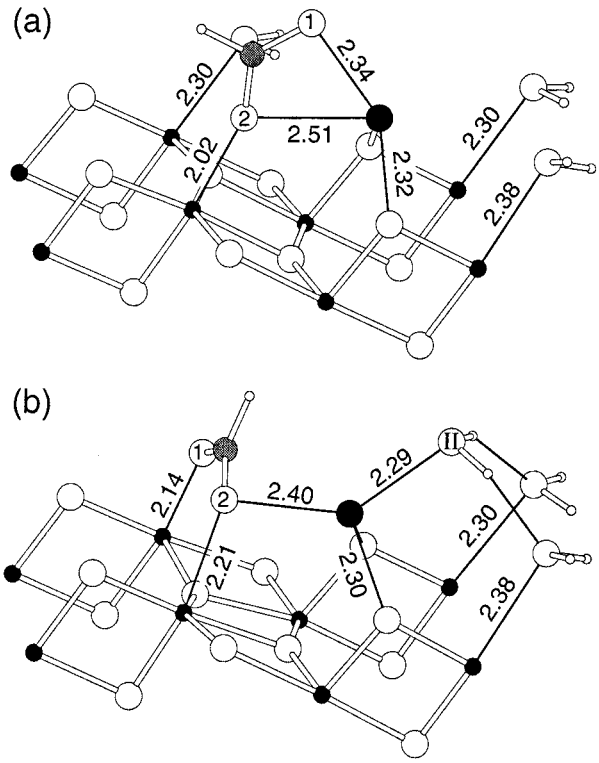

Figure 10. Same as Figure 9, for HCOONa co-adsorbed with three water molecules.

TABLE 3: Adsorption Energies (eV), Bond Distances (Å), and Bond Angles (deg) for the Monodentate (M) and Bridging Bidentate (BB) Conformations of HCOOH and HCOONa Co-Adsorbed with Three Water Molecules in a Supercell Containing Four Ti_{5c} Surface Sites[a]

geometry	figure	C−O1	C−O2	O1−C−O2	adsorption energy
M(H)−H_2O	9a	1.28	1.27	127.2	1.00
BB(H)−H_2O	9b	1.27	1.29	128.7	0.65
MNa−H_2O	10a	1.25	1.30	122.8	1.11
BBNa−H_2O	10b	1.27	1.29	129.0	1.75

[a] For the monodentate species, all H_2O molecules are coordinated to Ti_{5c} cation sites, while for the BB species one of the water molecules is part of the second layer.

the MNa and BBNa configurations on the dry surface (see Table 2). Thus the most stable geometry for the formate anion at the surface is the bridging one also when water is co-adsorbed.

Comparison between the structural parameters in Tables 2 and 3, as well as between the adsorption structures for the dry surface in Figures 4 and 5 and the corresponding ones for the hydrated surface in Figures 9 and 10, shows that modifications induced by the interactions with the co-adsorbed water molecules are more important for the acid than for the formate. For instance M(H)−H_2O (see Figure 9a), which is obtained starting from the molecular MHa conformation in Figure 4a, is an ester-type dissociated formate species, forming an H-bond with a surface-bridging group: due to the formation of a hydrogen bond between the hydroxy oxygen of MHa and a nearby water molecule, the proton of the acid is transferred to a surface O_{2c} site. Similarly, in BB(H)-H_2O, the proton forming a surface hydroxyl on the dry surface (see Figure 4b) is transferred to a water molecule, which then becomes a H_3O^+ species (see Figure 9b), confirming the weak basicity of O_{2c} surface sites.

The net adsorption energy of the formate species from an aqueous solution can be evaluated by adding the energies

involved in the processes (1) and (2), which yields a value of 0.79 eV. In this process, two water molecules, initially in contact with the surface, are displaced to outer layers. Vice versa, the adsorption energy for HCOOH has a value of only 0.30 eV, arising from process (1). Taking into account the uncertainties related to our simplified model of the hydrated surface, as well as to our restricted sampling of configurations for the investigated systems, we cannot exclude that such a monodentate $M(H)-H_2O$ structure may be actually unstable. Instead, the calculated bridging bidentate $BBNa-H_2O$ structure should account for the experimental ATR-FTIR observation of adsorbed $HCOO^-$ on anatase in contact with a slightly acidic solution.[13]

V. Conclusions

We have studied the adsorption of formic acid and sodium formate on the dry and hydrated TiO_2 anatase (101) surfaces via first principles density functional calculations in a slab geometry. For HCOOH, we find that a molecular monodentate species hydrogen bonded to a surface two-fold coordinated oxygen is preferred on the dry surface. This result is compatible with experiments of gaseous formic acid adsorption on anatase mixed (101)/(100) samples[13] and powders,[12] and confirms our previous finding of a rather low reactivity of the (101) anatase surface.[14,44] Moreover, since a dissociated bridging bidentate geometry is known to be the most stable for HCOOH on rutile (110), our result confirms the essential role of surface structure in determining the adsorption mode of a molecule.

Concerning HCOONa adsorption, a bridging bidentate geometry is strongly favored on the dry surface. This suggests that the greater stability of the monodentate with respect to the bridging bidentate structure for HCOOH should be largely related to the weak basicity of the O_{2c} sites on anatase (101). Bidentate chelating structures are not energetically stable neither for sodium formate, nor for formic acid.

Our calculations for the hydrated anatase surface indicate that both formic acid and sodium formate tend to form a specific inner-sphere coordination. For the formate, the bridging bidentate structure is again favored, with a net adsorption energy of 0.79 eV. For the acid, the preferred structure is a monodentate dissociated geometry which is stabilized by a hydrogen bond to a surface hydroxyl. However, the estimated net adsorption energy of 0.30 eV is rather small, particularly if we take into account the uncertainties related to our simplified model for the hydrated surface. This suggests that the adsorbed $HCOO^-$ species identified by ATR-FTIR experiments on hydrated anatase surfaces should rather have a bridging bidentate structure.

Acknowledgment. The calculations presented in this work have been performed on the NEC-SX4 of the CSCS at Manno (Switzerland). We thank J. M. Kesselman-Truttman et al. for sharing their ATR-FTIR results.

References and Notes

(1) Linsebigler, A. L.; Lu, G.; Yates, J. T. *Chem. Rev.* **1995**, *95*, 735.
(2) Hadjiivanov, K. I.; Klissurski, D. G. *Chem. Soc. Rev.* **1996**, *25*, 61.
(3) O'Regan, B.; Grätzel, M. *Nature (London)* **1991**, *353*, 737; Hagfelt, A.; Grätzel, M. *Chem. Rev.* **1995**, *95*, 49.
(4) Oliver, P. M.; Watson, G. W.; Kelsey, E. T.; Parker, S. C. *J. Mater. Chem.* **1997**, *7*, 563.
(5) Burnside, S. D.; Shklover, V.; Barbé, C.; Comte, P.; Arendse, F.; Brooks, K.; Grätzel, M. *Chem. Mater.* **1998**, *10*, 2419.
(6) Onishi, H.; Aruga, T.; Iwasawa, Y. *J. Am. Chem. Soc.* **1993**, *115*, 10460.
(7) Fukui, K.; Onishi, H.; Iwasawa, Y. *Chem. Phys. Lett.* **1997**, *280*, 296.
(8) Chambers, S. A.; Tevuthasan, S.; Kim, Y. J.; Herman, G. S.; Wang, Z.; Tober, E.; Ynzunza, R.; Morais, J.; Peden, C. H. F.; Ferris, K.; Fadley, C. S. *Chem. Phys. Lett.* **1997**, *267*, 51.
(9) Bates, S. P.; Kresse, G.; Gillan, M. J. *Surf. Sci.* **1998**, *409*, 336.
(10) Ahdjoudj, J.; Minot, C. *Catal. Lett.* **1997**, *46*, 83.
(11) Munuera, G.; Gonzalez, F.; Moreno, F.; Prieto, J. A. In *Catalysis: Proceedings of the 5th International Congress on Catalysis*; Hightower, J. W., Ed.; North Holland: Amsterdam, 1973; Vol. 2, p 1159.
(12) Kim, K. S.; Barteau, M. A. *Langmuir* **1988**, *4*, 945.
(13) Kesselman-Truttman, J. M.; Hug, S. J.; Rotzinger, F. P.; Shklover, V.; Grätzel, M. To be published.
(14) Vittadini, A.; Selloni, A.; Rotzinger, F. P.; Grätzel, M. *Phys. Rev. Lett.* **1998**, *81*, 2954.
(15) Lindan, P. J. D.; Harrison, N. M.; Holender, J. M.; Gillan, M. J. *Phys. Rev. Lett.* **1998**, *80*, 762.
(16) Bates, S. P.; Gillan, M. J.; Kresse, G. *J. Phys. Chem. B* **1998**, *102*, 2017.
(17) Car, R.; Parrinello, M. *Phys. Rev. Lett.* **1985**, *55*, 2741.
(18) Pasquarello, A.; Laasonen, K.; Car, R.; Lee, C.; Vanderbilt, D. *Phys. Rev. Lett.* **1992**, *69*, 1982; Laasonen, K.; Pasquarello, A.; Car, R.; Lee, C.; Vanderbilt, D. *Phys. Rev. B* **1993**, *47*, 10142.
(19) Perdew, J. P.; Chevary, J. A.; Vosko, S. H.; Jackson, K. A.; Singh, D. J.; Fiolhais, C. *Phys. Rev. B* **1992**, *46*, 6671.
(20) Dal Corso, A.; Pasquarello, A.; Baldereschi, A.; Car, R. *Phys. Rev. B* **1996**, *53*, 1180.
(21) Langel, W.; Parrinello, M. *Phys. Rev. Lett.* **1994**, *73*, 504; *J. Chem. Phys.* **1995**, *103*, 3240.
(22) Vanderbilt, D. *Phys. Rev. B* **1990**, *41*, 7892.
(23) Almenningen, A.; Bastiansen, O.; Motzfeldt, T. *Acta Chem. Scand.* **1969**, *23*, 2848.
(24) Szymanski, M. S.; Gillan, M. J. *Surf. Sci.* **1996**, *367*, 135.
(25) Goddard, J. D.; Yamaguchi, Y.; Schaefer, H. F., III. *J. Chem. Phys.* **1992**, *96*, 1158; Borisenko, K. B.; Bock, C. W.; Hargittai, I. *J. Mol. Struct. (THEOCHEM)* **1995**, *332*, 161; Turi, L. *J. Phys. Chem.* **1996**, *100*, 11285; Quian, W.; Krimm, S. *J. Phys. Chem. A* **1998**, *102*, 659.
(26) Nahringbauer, I. *Acta Crystallogr. B* **1978**, *34*, 315; Bjarnov, E.; Hocking, W. M. *Z. Naturforsch.* **1978**, *33A*, 610; Pettersson, M.; Lundell, J.; Khriachtchev, L.; Räsänen, M. *J. Am. Chem. Soc.* **1997**, *119*, 11715.
(27) Chao, J.; Zwolinski, J. *J. Phys. Chem. Ref. Data* **1978**, *7*, 863.
(28) Ramamoorthy, M.; Vanderbilt, D.; King-Smith, R. D. *Phys. Rev. B* **1994**, *49*, 16721.
(29) Goniakowski, J.; Holender, J. M.; Kantorovich, L. N.; Gillan, M. J.; White, J. A. *Phys. Rev. B* **1996**, *53*, 957.
(30) Cotton, F. A.; Wilkinson, G. *Advanced Inorganic Chemistry*, 5th ed.; Interscience: New York, 1988.
(31) Nakatsuji, H.; Yoshimoto, M.; Umemura, Y.; Takagi, S.; Hada, M. *J. Phys. Chem. B* **1996**, *100*, 694.
(32) Bartmess, J. E.; McIver, R. T., Jr. In *Gas Phase Ion Chemistry*; Bowers, M. T., Ed.; Academic: New York, 1979; Vol. 2.
(33) Redhead, P. A. *Vacuum* **1962**, *12*, 203.
(34) Truong, C. M.; Wu, M.-C.; Goodman, D. W. *J. Chem. Phys.* **1992**, *97*, 9447; Dilara, P. A.; Vohs, J. M. *J. Phys. Chem.* **1993**, *97*, 12919.
(35) Gautier-Luneau, I.; Mosset, A.; Galy, J. *Z. Kristallogr.* **1987**, *180*, 83; Doeuff, S.; Dromzee, Y.; Tauelle, F.; Sanchez, M. *Inorg. Chem.* **1989**, *28*, 4439.
(36) We used the Amsterdam Density Functional package; Version 2.3.0; Vrije Universiteit: Amsterdam, The Netherlands, 1997. See also: Baerends, E. J.; Ellis, D. E.; Ros, P. *Chem. Phys.* **1973**, *2*, 41; te Velde, G.; Baerends, E. J. *J. Comp. Phys.* **1992**, *99*, 84; Fonseca Guerra, C.; Visser, O.; Snijders, J. G.; Baerends, E. J. In *Methods and Techniques in Computational Chemistry*; Clementi, E., Corongiu, G., Eds.; STEF: Cagliari, 1995; p 305.
(37) Calculations were done using a triple-ζ STO basis set for Ti, and a double-ζ basis set, with an extra polarization function, for C, O, and H atoms. GGA corrections were of the same type used for the slab calculations. The cluster embedding was provided by pseudo-hydrogen saturators.[38]
(38) Casarin, M.; Maccato, C.; Vittadini, A. *J. Phys. Chem. B* **1998**, *102*, 10745.
(39) In these calculations a compensating uniform background of charge was used.
(40) Cluster calculations (San Miguel, M. A.; Calzado, C. J.; Sanz, J. F. *Surf. Sci.* **1998**, *409*, 92) have found a similar geometry for sodium on the rutile (110) surface.
(41) Zachiaresen, W. H. *J. Am. Chem. Soc.* **1940**, *62*, 1011; Markila, P. L.; Rettig, S. J.; Trotter, J. *Acta Crystallogr. B* **1975**, *31*, 2927; Müller, K.; Range, K.-J.; Heyns, A. M. *Z. Naturforsch.* **1994**, *49b*, 1179.
(42) Eichinger, M.; Tavan, P.; Hutter, J.; Parrinello, M. *J. Chem. Phys.* **1999**, *110*, 10452.
(43) Since four Ti_{5c} sites are present in our supercell, one monolayer can accomodate either a singly-coordinated formate co-adsorbed with three water molecules, or a bridging bidentate species co-adsorbed with two H_2O molecules (or, else, four water molecules).
(44) Selloni, A.; Vittadini, A.; Grätzel, M. *Surf. Sci.* **1998**, *402-404*, 104.